Journal of Cell Science 110, 409-420 (1997)
Printed in Great Britain © The Company of Biologists Limited 1997
JCS1323

Dimples, pores, star-rings, and thin rings on growing nuclear envelopes: evidence for structural intermediates in nuclear pore complex assembly

Martin W. Goldberg[1,*], Christiane Wiese[2,*], Terence D. Allen[1] and Katherine L. Wilson[2,†]

[1]CRC Department of Structural Cell Biology, Paterson Institute for Cancer Research, Christie Hospital National Health Service Trust, Manchester, M20 9BX, UK
[2]Department of Cell Biology and Anatomy, The Johns Hopkins University School of Medicine, 725 North Wolfe Street, Baltimore, Maryland 21205, USA

*Both authors contributed equally to this work
†Author for correspondence (e-mail: Kathy_Wilson@qmail.bs.jhu.edu)

SUMMARY

We used field emission in-lens scanning electron microscopy to examine newly-assembled, growing nuclear envelopes in *Xenopus* egg extracts. Scattered among nuclear pore complexes were rare 'dimples' (outer membrane depressions, 5-35 nm diameter), more abundant holes (pores) with a variety of edge geometries (35-45 nm diameter; 3.3% of structures), pores containing one to eight triangular 'star-ring' subunits (2.1% of total), and more complicated structures. Neither mature complexes, nor these novel structures, formed when wheat germ agglutinin (which binds *O*-glycosylated nucleoporins) was added at high concentrations (>500 μg/ml) directly to the assembly reaction; low concentrations (10 μg/ml) had no effect. However at intermediate concentrations (50-100 μg/ml), wheat germ agglutinin caused a dramatic, sugar-reversible accumulation of 'empty' pores, and other structures; this effect correlated with the lectin-induced precipitation of a variable proportion of each major *Xenopus* wheat-germ-agglutinin-binding nucleoporin. Another inhibitor, dibromo-BAPTA (5,5′-dibromo-1,2-bis[o-aminophenoxy]ethane-N,N,N′,N′-tetraacetic acid), had different effects depending on its time of addition to the assembly reaction. When 1 mM dibromo-BAPTA was added at time zero, no pore-related structures formed. However, when dibromo-BAPTA was added to growing nuclei 40-45 minutes after initiating assembly, star-rings and other structures accumulated, suggesting that dibromo-BAPTA can inhibit multiple stages in pore complex assembly. We propose that assembly begins with the formation and stabilization of a hole (pore) through the nuclear envelope, and that dimples, pores, star-rings, and thin rings are structural intermediates in nuclear pore complex assembly.

Key words: Nuclear pore complex, Nuclear envelope, FEISEM

INTRODUCTION

The nuclear envelope consists of two concentric membranes (outer and inner), which enclose a lumenal space continuous with the ER lumen (reviewed by Wilson and Wiese, 1996). Molecules move across the nuclear envelope through nuclear pore complexes (NPCs). Ions and small molecules diffuse through aqueous channels associated with the NPC, but molecules larger than ~40 kDa, as well as many smaller nuclear proteins such as histones, are recognized and transported through the NPC by active mechanisms (reviewed by Hicks and Raikhel, 1995; Görlich and Mattaj, 1996).

NPC structure has been revealed by a variety of electron microscopy techniques (Maul, 1977a; Reichelt et al., 1990; Ris, 1991; Jarnik and Aebi, 1991; Goldberg and Allen, 1992; Hinshaw et al., 1992; Akey and Radermacher, 1993; Panté and Aebi, 1993). The inner and outer nuclear membranes are continuous around each NPC, creating a ~70 nm hole or 'pore' through the nuclear envelope (Maul, 1977a). Within this pore sits the NPC, which has a mass of ~120 mega Daltons (Reichelt et al., 1990). The NPC is thought to be anchored to the pore membrane by integral proteins: candidates are gp210 (16-24 copies per NPC; Gerace et al., 1982) and POM121 (Hallberg et al., 1993) in mammals, and POM152 in yeast (Wozniak et al., 1994). In general, NPC structure consists of three stacked rings (Reichelt et al., 1990; Ris, 1991; reviewed by Rout and Wente, 1994; Akey, 1995; Davis, 1995; Goldberg and Allen, 1995): the cytoplasmic ring (which sits on the outer nuclear membrane), the nucleoplasmic ring (which sits on the inner nuclear membrane), and the central transporter and 'spoke' ring complex (which extends laterally into the pore membrane). The three rings are interconnected by vertical supports. Each ring has prominent eightfold symmetry when viewed from the cytoplasmic or nucleoplasmic side. Eight fibers extend from the cytoplasmic ring into the cytoplasm; these fibers contain the large Ran-binding protein, RBP2, and are thought to help capture import substrates (reviewed by Görlich and Mattaj, 1996). A different set of eight fibers extends from the nucleoplasmic ring into the nucleus, and are joined at their distal ends to form a 'basket' structure (Ris,

1991; Jarnik and Aebi, 1991; Goldberg and Allen, 1992). The basket may mediate nuclear export: for example, during their export from *Chironomus* salivary gland nuclei, large RNP particles known as Balbiani rings first contact the NPC at the basket (Kiseleva et al., 1996).

Each NPC is thought to consist of about 1,000 polypeptides, termed nucleoporins. Because NPCs have both eight-fold and two-fold structural symmetry, each NPC is estimated to consist of multiple copies of ~100 distinct nucleoporins (Rout and Blobel, 1993). About twenty nucleoporins have been identified so far (Rout and Wente, 1994).

Pore complexes disassemble during mitosis in higher eukaryotes (Maul, 1977a,b; reviewed by Macaulay and Forbes, 1996a; Davis, 1995), along with the nuclear membranes and lamina (reviewed by Georgatos et al., 1994; Wilson and Wiese, 1996). Except for the integral membrane proteins, most identified nucleoporins are released from the membrane and become soluble during mitosis. Some nucleoporins, such as p62, can be isolated as multisubunit complexes from mitotic *Xenopus* egg cytosol, suggesting that they retain structural contacts with other nucleoporins when NPCs are disassembled (Dabauvalle et al., 1990; Finlay et al., 1991; Macaulay et al., 1995).

The reconstruction of the NPC after mitosis is an interesting three-dimensional puzzle (reviewed by Macaulay and Forbes, 1996a). Although the mechanism of pore complex assembly has remained speculative, several important principles have been established. First, mitotically-disassembled NPC subunits appear to be recycled to build new NPCs on the daughter nuclei, since inhibitors of protein synthesis have no effect on the total number of NPCs that form by mid-G_1 phase (Maul et al., 1973). Second, NPC assembly is largely independent of chromatin and the nuclear lamina. This assertion is based on two sets of observations: functional NPCs can assemble in nuclear envelopes that lack a lamina (although basket structures were occasionally found on the wrong side of the envelope, suggesting that the lamina may directly or indirectly help orient NPCs; Goldberg et al., 1995), and NPCs can assemble into membranous structures named annulate lamellae, both in vivo (Kessel, 1992) and in vitro (Dabauvalle et al., 1991; Meier et al., 1995; see also Allan and Vale, 1994). Annulate lamellae are thought to be a storage compartment for NPCs and nuclear membranes, and typically form in oocytes and transformed cells. Although the NPCs that assemble in annulate lamellae include the Wheat Germ Agglutinin (WGA)-binding nucleoporins (Dabauvalle et al., 1991; Meier et al., 1995; Cordes et al., 1995), it is not known if these NPCs are functional. For example, NPC substructures found only on the nuclear side of the NPC, such as the basket, may not assemble correctly on annulate lamellae. Finally, because the number of NPCs doubles during interphase when the nucleus remains intact (Maul, 1977a), and because nuclear envelopes do not disassemble in lower eukaryotes, it has long been thought that a mechanism must exist to add new NPCs, and their corresponding pores/holes, to pre-existing nuclear envelopes. Using an in vitro assay, Macaulay and Forbes (1996b) demonstrated that NPC assembly requires the prior assembly of a double nuclear membrane. Furthermore, NPC assembly can be inhibited at early stages by GTPγS and BAPTA (1,2-bis[o-aminophenoxy]ethane-N,N,N′,N′-tetraacetic acid; a Ca^{2+} and Zn^{2+} buffer), as assayed by the lack of immunofluorescence when nuclei are stained with a monoclonal antibody (mAb 414) that recognizes the XFXFG-repeat class of nucleoporins (Macaulay and Forbes, 1996b; reviewed by Rout and Wente, 1994).

Nuclei assembled in *Xenopus* egg extracts are structurally normal and competent for DNA replication (Lohka and Masui, 1984; reviewed by Lohka, 1988; Hutchison et al., 1994; Wilson and Wiese, 1996) and RNA polymerase III transcription (Ullman and Forbes, 1995). We examined the surface of nuclei growing in *Xenopus* extracts using field emission in-lens scanning electron microscope (FEISEM; reviewed by Allen and Goldberg, 1993), which has a resolution comparable to that of the transmission electron microscope. Because we were interested in the behavior of nuclear vesicles and membranes during assembly, our fixation conditions were optimized for membrane preservation. The FEISEM analysis reported here revealed novel structures in the growing nuclear envelope, which we named ‘dimples’ and ‘stabilizing pores’, as well as pores (holes) that contained structures previously identified as subunits of mature NPCs: star-rings (Goldberg and Allen, 1996), and thin rings (E. Kiseleva and T. D. Allen, unpublished data). Experiments with WGA and BAPTA suggested that the stabilizing pores and star-rings may be structural intermediates in NPC assembly.

MATERIALS AND METHODS

Buffers and reagents

Membrane wash buffer (MWB): 250 mM sucrose, 50 mM KCl, 2.5 mM $MgCl_2$, 10 mM Hepes, pH 7.4, 2 mM DTT, 1 μg/ml leupeptin, 1 μg/ml aprotinin. Saltwash buffer: 1.2 M KCl, 250 mM sucrose, 10 mM Tris-HCl, pH 8.5, 2.5 mM $MgCl_2$, 2 mM DTT, 12 mM EDTA. Demembranated *Xenopus* sperm chromatin was prepared as described (Lohka and Masui, 1983; Newmeyer and Wilson, 1991). 5,5′-dibromo-BAPTA, the most potent BAPTA derivative tested by Sullivan et al. (1993), was from Molecular Probes, Inc. (Eugene, OR). Wheat germ agglutinin (WGA) was purchased from Sigma, and stored as 10 mg/ml stocks at −80°C.

Nuclear assembly reactions

Xenopus egg extracts were fractionated as described (Newmeyer and Wilson, 1991), except that our membrane wash buffer (MWB) lacked ATP. We first discovered the structures reported here while examining nuclear envelopes that had been assembled using salt-washed membranes; saltwashing removes most membrane-bound ribosomes and thereby makes NPCs more obvious. However, these structures were also present on nuclei assembled with non-saltwashed membranes (see Fig. 2). The use of saltwashed membranes had no adverse effect on nuclear assembly or structure. Saltwashing: fresh membranes were washed once in MWB, resuspended in saltwash buffer, incubated on ice for 30 minutes, pelleted, washed in MWB, frozen in liquid N_2, and stored at −80°C. For typical nuclear assembly reactions, frozen/thawed components (18 μl cytosol, 1 μl salt-washed membranes, and 1 μl demembranated sperm chromatin, final concentration 2,000 per μl) were mixed on ice and incubated at 22-24°C.

In assembly reactions that contained WGA, WGA was added to the reaction mixture on ice and either centrifuged immediately, or incubated at 22-24°C for 30 minutes before centrifuging. In reactions that contained dibromo-BAPTA, nuclear assembly was allowed to proceed for 45-50 minutes before dibromo-BAPTA was added to 1 mM final concentration from a 10 mM stock; samples were further incubated for 1 hour before processing for FEISEM.

Sample processing for FEISEM

After 40 minutes of incubation, a 4 μl aliquot was diluted with 1 ml modified MWB (modifications: pH 7.4, 150 mM sucrose), centrifuged

onto silicon chips (800 ***g***; Allen and Goldberg, 1994), fixed 10 minutes in 150 mM sucrose, 80 mM Pipes-KOH, pH 6.8, 1 mM $MgCl_2$, 2% paraformaldehyde, 0.25% glutaraldehyde, and then postfixed in 1% OsO_4 buffered in 0.2 M cacodylate, pH 7.4. Further processing and FEISEM analysis were as described by Goldberg and Allen (1992). These fixation conditions did not prevent NPC shrinkage as well as fixatives that contained tannic acid. However, tannic acid was omitted here because it caused artifactual membrane vesiculation (C. Wiese and M. W. Goldberg, unpublished observations). The structures reported here are also seen in assembling nuclear envelopes prepared by other fixation conditions, including those containing tannic acid.

Gels and WGA-blots

Tubes containing 9 µl cytosol (~270 µg protein) on ice were supplemented with 1 µl WGA to final WGA concentrations of 10, 50, 100, or 500 µg/ml. Samples were either immediately centrifuged at 14,000 ***g*** for 10 minutes at 4°C, or incubated for 30 minutes at 22-24°C before centrifuging. One-third of each pellet and supernatant were subjected to SDS-PAGE, blotted to PVDF, blocked for at least one hour at 37°C in buffer containing 0.2% SDS and 1 mg/ml hemoglobin, and probed with biotinylated WGA (Pierce) followed by Extravidin-conjugated alkaline phosphatase (Sigma). A separate dilution series was used to determine the linear range of alkaline phosphatase reaction product, and blots were scanned to estimate the relative amount of each band in the pellet.

RESULTS

To assemble functional nuclei in vitro, the cytosol and membrane fractions of *Xenopus* egg extracts were reconstituted with demembranated sperm chromatin. In some experiments

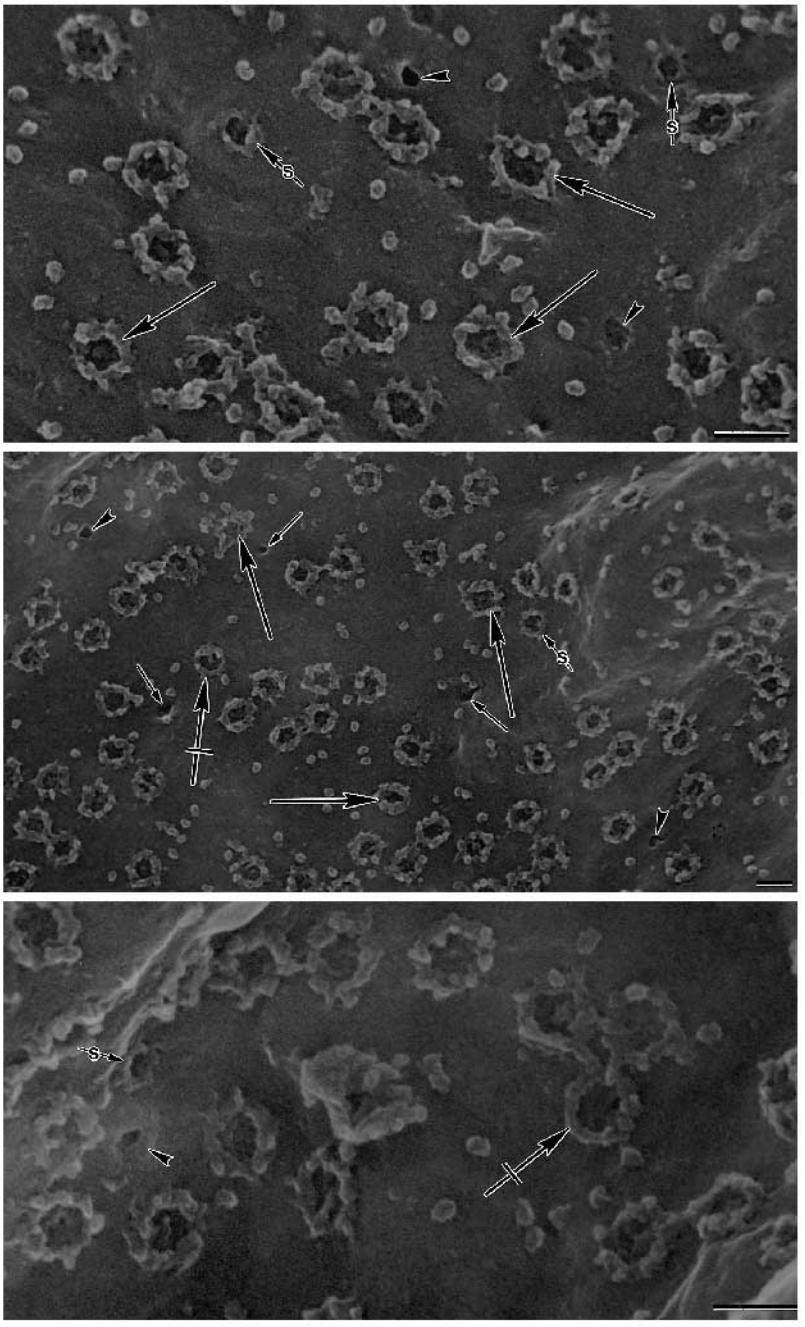

Fig. 1. The cytoplasmic surface of in vitro-assembled nuclear envelopes visualized by FEISEM. Nuclear envelopes were fixed 40 minutes after initiating assembly, when nuclei were enclosed within a double membrane and actively growing. Mature NPCs (large arrows), dimples (small arrows), stabilizing pores (arrowheads), star-rings (arrows marked 's'), and late intermediates (crossed arrows). Bars, 100 nm.

the membranes were prewashed with 1.2 M KCl to remove the majority of ribosomes. Salt treatment has no detectable effect on nuclear envelope assembly or nuclear growth (Wilson and Newport, 1988), but improved our view of the nuclear membrane surface. At various timepoints during assembly the nuclei were diluted into MWB and centrifuged onto silicon chips, where they were fixed and processed for scanning microscopy. The FEISEM analysis of nuclear envelope assembly, which is reported in detail elsewhere (C. Wiese et al., unpublished), showed that vesicles rapidly bound and flattened onto the chromatin surface, and that mature NPCs first became visible within 8 minutes. Initially, few NPCs were observed. However, after 40 minutes of incubation the growing nuclei had accumulated many mature NPCs (Fig. 1).

The structure of mature in vitro-assembled NPCs is consistent with previous findings

The mature NPCs in Fig. 1 had an external diameter of ~105 nm, which was slightly smaller than that previously reported for *Xenopus* oocyte NPCs (110 nm; Goldberg and Allen, 1993), but consistent with the diameter of the cytoplasmic ring reported for unfixed oocyte NPCs rapidly frozen and embedded in thin ice (105 nm, if lumenal mass is excluded; Akey and Radermacher, 1993). The fixation conditions used here, which were based on those of Allan and Vale (1994), were designed to optimally preserve membranes. The structure of mature NPCs under these conditions was consistent with that previously reported (Goldberg and Allen, 1993) and identical to *Xenopus* oocyte NPCs fixed in the same way (data not shown). The cytoplasmic ring of mature NPCs, which consists of eight bipartite subunits, was decorated with eight particles that we assumed are collapsed cytoplasmic fibers (Fig. 1). Internal structures were also visible, but could not be resolved clearly.

Characterization of novel membrane and protein structures

At the 40 minute timepoint many NPCs had assembled on the nuclear envelope, as viewed by FEISEM from the cytoplasmic side. Scattered among the mature NPCs were a number of membrane dimples (Fig. 1, small arrows) and holes (Fig. 1, arrowheads), and other structures including star-rings (Fig. 1, arrows marked S) and thin rings (Fig. 1, crossed arrows). These

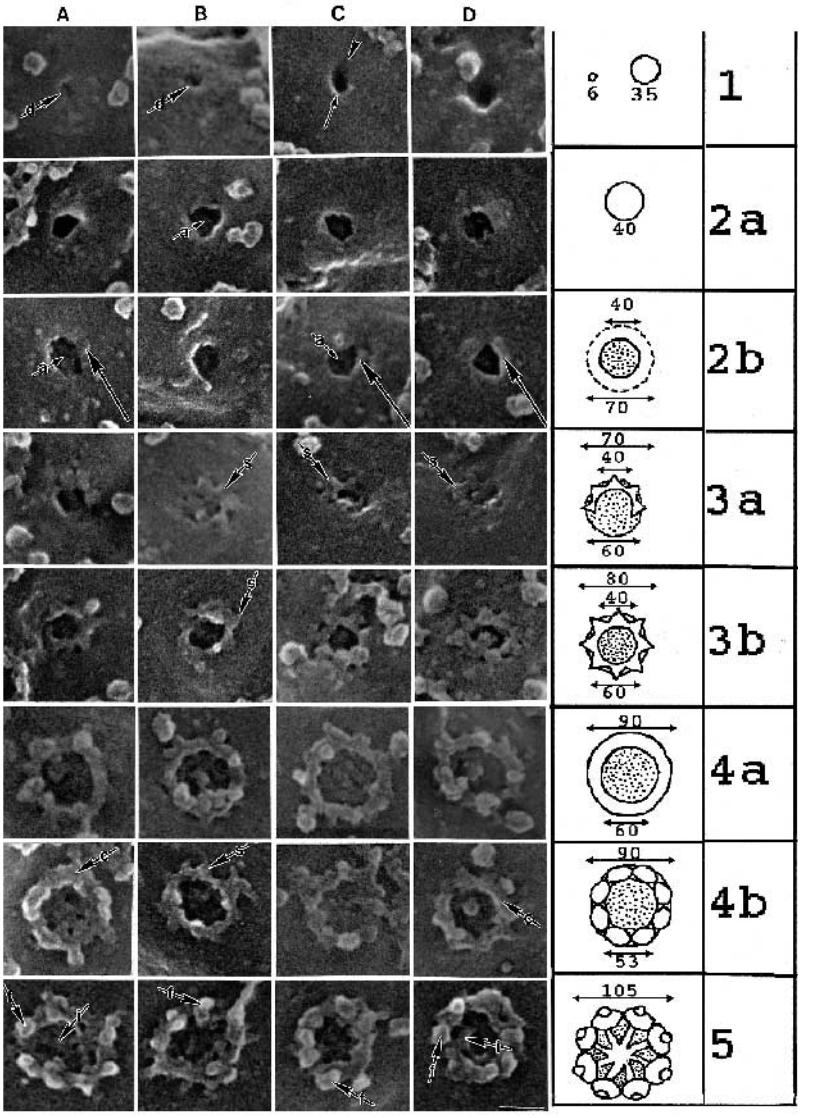

Fig. 2. Examples of dimples, 'stabilizing pores', star-rings, thin rings, and more complicated NPC structures. Each row shows four examples of a given structure, with the most 'mature' (complete) examples to the right, plus an enface diagram of the complete structure. The examples shown were assembled using both saltwashed and non-saltwashed membranes. (Row 1) Dimples. (Rows 2a and 2b) 'Stabilizing pores'. (Rows 3a and 3b) Star-rings. (Rows 4a and 4b) Thin rings, and thin rings with additional uncharacterized mass. (Row 5) Nearly-mature NPCs, which have central NPC structures and up to eight globular particles, presumed to be collapsed cytoplasmic filaments. Small arrows indicate sharp edge of dimple; arrowheads, gently sloping edge of dimple; large arrows, putative hole stabilizing material. Other arrows are marked as follows: d, dimple; a, central material, s, subunits of star-ring; c, cytoplasmic coaxial ring; f, cytoplasmic filaments; i, internal structures. Bar, 50 nm.

Table 1. Estimated frequency of novel structures at 40 minutes of assembly

NPC stage	Number	% of total
Dimples	7	0.6
Stabilising pores	42	3.3
Star-rings	27	2.1
All others + mature NPCs	1197	94

structures represented a small fraction of the total NPCs (Table 1): holes (3.3%) were more abundant than dimples (0.6%) or star-rings (2.1%). The dimples and holes were always smaller than the ~70 nm pores in which mature NPCs reside. We grouped these structures into five classes of increasing size and complexity, as follows (Fig. 2).

Dimples or depressions in the outer nuclear membrane

Dimples had smooth, rounded edges and no obvious structure within the depression (Fig. 2, row 1). They ranged in diameter from ~6-35 nm, and were typically under 20 nm; dimples larger than 20 nm in diameter were difficult to distinguish from pores (see below). Dimples were often asymmetric, with one side appearing to slope gently towards the deepest part (arrowhead), whereas the other side had a sharper edge presumably because it was more highly curved (small arrow). This variable geometry, and the lack of obvious structure in the center, suggested that dimpling may be initiated and maintained by proteins within the nuclear envelope lumen. Dimples were relatively rare (Table 1), suggesting that they were short-lived.

Pores (holes) with a variety of edge geometries

'Holes' or pores with a diameter of 35-45 nm were relatively abundant (Table 1). These structures had sharp edges and irregular, often angular shapes, suggestive of partially-assembled hole-stabilizing structures near the membrane. We collectively named them 'stabilizing pores'. The sharp appearance of the edges could be explained in two ways: either the membrane was highly curved as it dipped into the hole, or there were protein structures associated with the cytoplasmic, lumenal, or both sides of the membrane. Indeed, some stabilizing pores (Fig. 2, row 2b) had a clearly increased secondary electron signal around their perimeter, creating what looked like a poorly-contrasted ring around the hole. High magnification stereo pair analysis (see Fig. 3A) showed that there was increased topographical contrast of the outer membrane, which could indicate structures too tightly associated with the cytoplasmic side of the membrane to be resolved. However, since FEISEM can also detect *sub*surface density (Allen and Goldberg, 1993), the ring signal might be due to a bulky subsurface structure, such as the large lumenal ring recently isolated from yeast NPCs (Strambio-de-Castillia et al., 1995).

One notable feature of the 'stabilizing pores' was their diversity of shapes, which ranged from almost triangular (Fig. 2, row 2b, right panel) to scalloped (Fig. 2, row 2a, two middle panels). This variety suggested that each pore was being stabilized by a slightly different, possibly random, order of assembly of the structural components that defined the edge.

Interestingly, the stabilizing pores had material across their centers (Fig. 2, rows 2a and 2b, arrows marked a). Stereo pairs

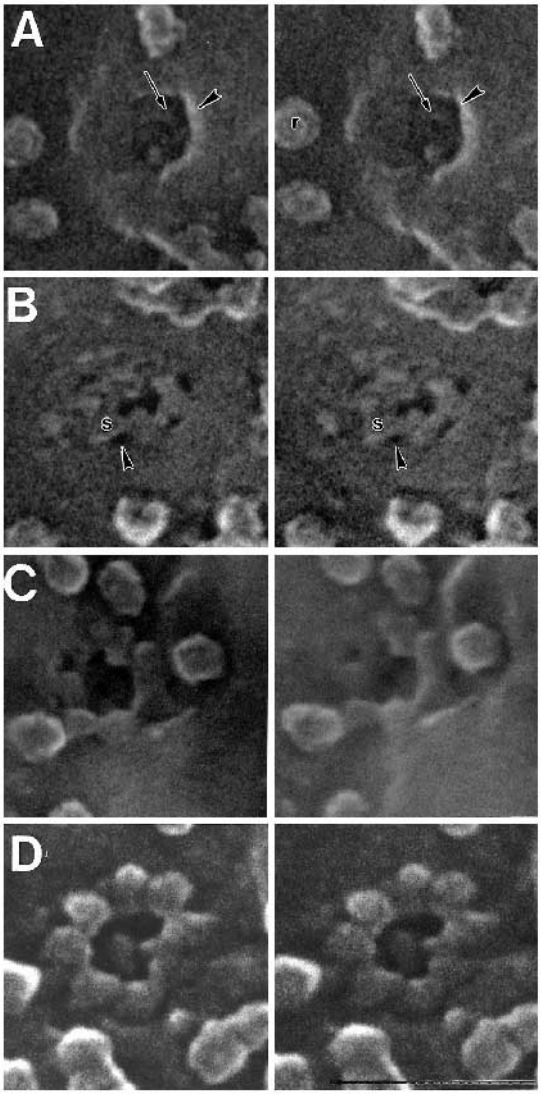

Fig. 3. Stereo pairs of a stabilized pore and three different star-rings. (A) The central structures (arrows) of the stabilized pore lie beneath the level of the outer membrane (arrowheads). (B) The subunits ('s') of the immature star-ring assemble within the pore (arrowheads) near the level of the membrane, but not above it. (C) Growth of individual star-ring modules, which rise above the plane of the outer membrane when completed. (D) Nearly-mature star-ring. Bar, 100 nm.

(Fig. 3A) showed that these central structures lay below the level of the outer membrane, and might therefore represent the assembling spoke ring complex or central transporter (Akey and Radermacher, 1993; Allen and Goldberg, 1995), or less possibly the nucleoplasmic basket (see Discussion). The relative abundance of the stabilizing pores (holes) suggested that the formation of a stable pore (and its central structures) might be a relatively lengthy process.

Modularly-assembling star-rings

Star-rings, which have eight triangular subunits, were recently discovered as a distinct substructure situated between the membrane and the cytoplasmic ring of oocyte NPCs (Goldberg and Allen, 1996). In our growing nuclear envelopes, we were intrigued to find some apparently mature star-rings in which

triangular subunits formed an eight-pointed structure (ID ~40 nm, OD ~80 nm) within pores of ~60 nm diameter (Fig. 2, row 3b, right). However, we also found many structures with fewer than eight subunits (Fig. 2, rows 3a and 3b), suggesting that star-rings assembled one subunit at a time. There were two types of star-ring subunits: the first type lay flat within the hole (Fig. 3B), and the second rose above the surface of the outer membrane (Fig. 3C,D). We hypothesized that the flat subunits were precursors to the tall subunits. In this view, star-ring assembly would start within the pore, level with the outer nuclear membrane, and each subunit would gradually build up and out to reach full height above the outer membrane. Interestingly, where measureable (e.g. compare in Fig. 2, row 2b versus row 3b columns A and C), the pores (holes) that contained star-rings were larger than the stabilizing pores (~60 nm versus 35-45 nm diameter).

Thin rings and cytoplasmic coaxial rings with uncharacterized central structures

Thin rings were smoother and larger (ID ~53 nm, OD ~90 nm) than star-rings, but smaller than the completed cytoplasmic ring (OD 105 nm). In some cases, star-ring subunits were visible below incomplete thin rings, suggesting that thin rings formed on top of the star-rings (Fig. 2, row 4b, arrow marked S). Many thin rings (Fig. 2, rows 4a and 4b) carried one or more additional bulkier subunits. Thin rings with a full array of bulky subunits (e.g. Fig. 2, row 4b, column A) looked like cytoplasmic coaxial rings. We concluded that the thin ring was a distinct substructure that served as the foundation for assembling the cytoplasmic coaxial ring.

Nearly-mature NPCs with additional central structures and up to eight collapsed cytoplasmic filaments

There were many NPC structures with cytoplasmic coaxial rings that appeared nearly mature, with an external diameter of ~105 nm, up to eight globular particles on top, and additional mass across the center (Fig. 2, rows 4b and 5). Due to their structural heterogeneity, these nearly-mature NPCs were difficult to characterize unambiguously. The globular particles on top of the cytoplasmic ring most likely correspond to collapsed cytoplasmic filaments, which were not optimally preserved under our fixation conditions. Some globular particles might be ribosomes, although we consider this unlikely because soluble ribosomes are substantially depleted from cytosol during extract preparation (ribosomes pellet at 200,000 ***g***; Lohka and Masui, 1984), and most but not all membrane-associated ribosomes were removed by salt-extraction (see Materials and Methods).

The dimples, pores, star-rings, and thin rings reported here were detectable throughout the course of the assembly reaction, starting as early as 10 minutes after initiating assembly, and under a variety of fixation conditions (data not shown). In contrast, dimples, pores, star-rings, and thin rings were never seen on similarly-prepared *Xenopus* oocyte nuclear envelopes (M. W. Goldberg, unpublished observations) which contain only mature NPCs. Furthermore, no changes in NPC morphology were seen when freshly-isolated nuclear envelopes from *Xenopus* oocytes were incubated in egg extracts for 60 minutes (J. M. Cronshaw and M. W. Goldberg, unpublished observations). Oocyte nuclear envelopes possess a nearly-crystalline array of mature NPCs (see Davis, 1995) which may leave little room to assemble new NPCs. More importantly, the absence of dimples, pores, star-rings, and thin rings from the extract-incubated oocyte nuclear envelopes indicates that these structures are not the result of extract-induced NPC breakdown.

Different concentrations of WGA block NPC assembly at different stages

We hypothesized that the above structures might be intermediates in NPC assembly, and tested this idea using two inhibitors of NPC assembly, WGA and BAPTA. Depleting the cytosol of WGA-binding nucleoporins has two published effects on nuclear assembly: either no NPCs form (Dabauvalle et al., 1990), or nonfunctional, structurally-abnormal NPCs form (Finlay and Forbes, 1990). We have reproduced both phenotypes in WGA-depleted cytosol (Wiese et al., unpublished). However, the effects of adding WGA directly to a nuclear assembly reaction had not previously been reported. When present at high concentrations (>500 μg/ml) in the assembly reaction, WGA completely inhibited NPC formation (Fig. 4A), with the occasional exception of aberrant NPCs; consistent with the lack of NPCs, these WGA-inhibited nuclei failed to grow (data not shown). We concluded that WGA binds to *O*-glycosylated nucleoporins that are either essential for initiating NPC assembly, or essential for stabilizing NPC formation at an early stage. Control reactions treated with a low concentration of WGA (10 μg/ml) formed many normal-appearing NPCs (Fig. 4D), and these nuclei grew (data not shown). We deduced that 10 μg/ml WGA was insufficient to bind all *O*-glycosylated targets. Many transcription factors and chromatin proteins are *O*-glycosylated (reviewed by Hart et al., 1989), and presumably compete with *O*-glycosylated nucleoporins for binding to WGA.

Interestingly, when assembly reactions contained intermediate concentrations of WGA (50-100 μg/ml), individual nuclei exhibited one of two phenotypes: they either accumulated stabilizing pores plus the other structures (plus mature-appearing NPCs; Fig. 4C), or they accumulated the stabilizing pores almost exclusively (Fig. 4B). Furthermore, the WGA-arrested pores appeared to lack the material usually found across the center and were therefore deemed ‘empty’. The common phenotype in all reactions containing either 50 or 100 μg/ml WGA was the accumulation of empty stabilizing pores. In two out of three such experiments, all nuclei accumulated empty pores, but a minority of nuclei also formed other NPC-related structures and mature NPCs. In one out of three experiments, the predominantly ‘empty pore’ nuclei (as seen in Fig. 4B) were outnumbered by the alternative phenotype. We concluded that WGA concentrations around 50-100 μg/ml allowed assembly to proceed to the ‘stabilizing pore’ stage, but blocked the formation of structures across the center of the pore (see Discussion), and also interfered with later stages of assembly. The accumulation of empty pores (and other putative intermediates) was completely reversed when the competing sugar, N,N′,N″-triacetylchitotriose (TCT) was added to WGA-inhibited reactions and the nuclei fixed and examined 60 minutes later (data not shown; other timepoints not tested). The empty pores were unlikely to be artifacts caused by WGA for three reasons: first, higher concentrations of WGA resulted in fewer pores (Fig. 4A), second, ER membranes found adjacent

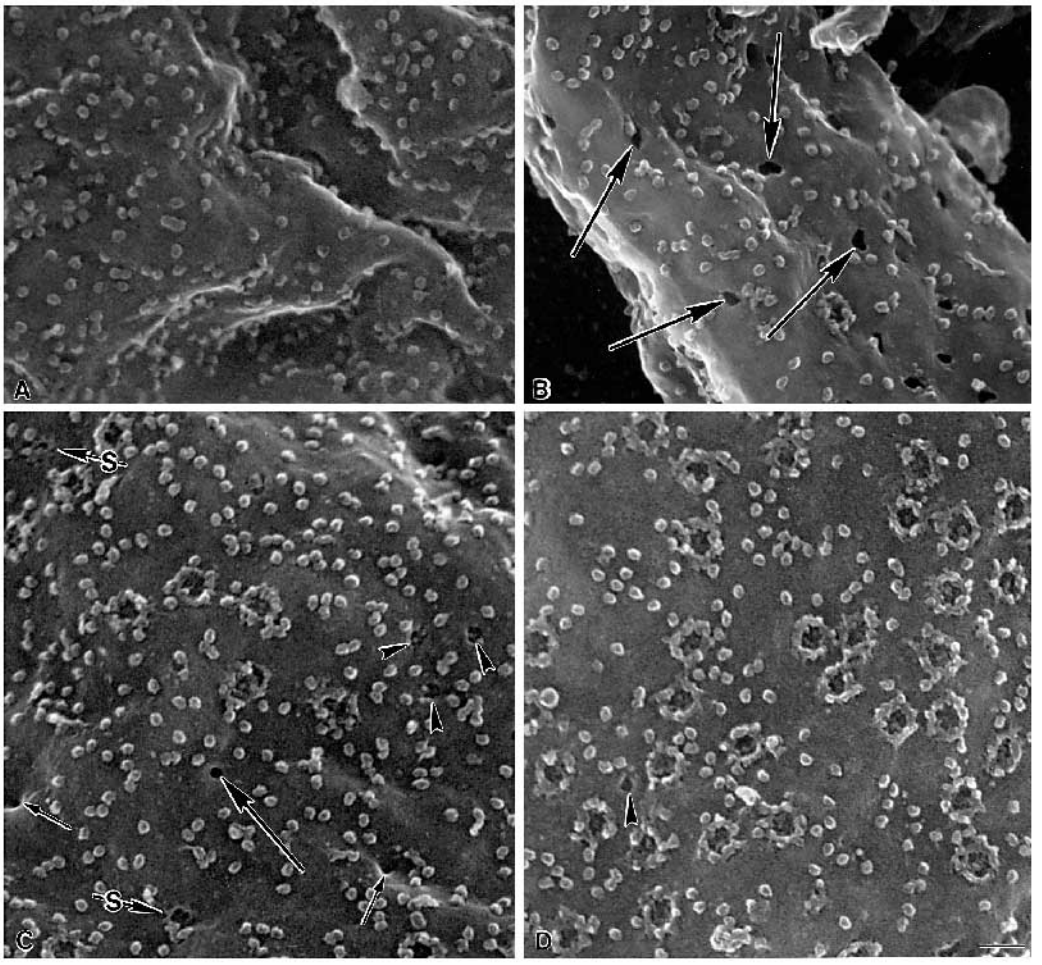

Fig. 4. WGA added directly to assembly reactions causes 'stabilizing pores' and other putative intermediates to accumulate. Nuclei were assembled for 60 minutes in the continuous presence of (A) high (500 μg/ml), (B, C) intermediate (50 and 100 μg/ml), and (D) low (10 μg/ml) concentrations of WGA, and then analyzed by FEISEM. At the intermediate concentrations (50-100 μg/ml), WGA caused empty stabilizing pores to accumulate predominantly (as shown in B), or empty pores accumulated along with other intermediates and mature NPCs (as shown in C). Nuclei with the phenotype shown in (B) predominated in two out of three experiments at both intermediate WGA concentrations. (Large arrows) 'empty' stabilizing pores; (arrowheads) normal stabilizing pores; (small arrows) dimples; (arrows marked s) star-rings. Bar, 100 nm.

to nuclei had no such pores (not shown), and finally, pore accumulation was reversed by adding the competing sugar. These results suggested that 'stabilizing pores' may be genuine intermediates in NPC assembly.

Why was the arrest point not uniform in reactions containing 50-100 μg/ml WGA? The predominant phenotype was the accumulation of empty stabilizing pores (holes), but each experiment always included some fraction of nuclei that had apparently 'broken through' this arrest point to form larger structures, including mature NPCs. To ask what happened when WGA was added directly to assembly reactions, WGA was added to cytosol on ice at final concentrations of 10, 50, 100, and 500 μg/ml, and either immediately centrifuged for 10 minutes at 14,000 ***g*** (data not shown), or incubated 30 minutes at 22-24°C before centrifuging (Fig. 5). Pellets (containing insoluble aggregates) and supernatants were subjected to SDS-PAGE, blotted, and probed with biotinylated WGA (Fig. 5). Low WGA concentrations, which had no effect on NPC formation, did not affect the solubility of WGA-binding nucleoporins. In contrast, high WGA concentrations caused all three major WGA-binding nucleoporins to pellet quantitatively, suggesting that they aggregated and precipitated almost immediately upon WGA addition. Interestingly, at intermediate WGA concentrations (50 and 100 μg/ml) a proportion of each WGA-binding nucleoporin became pelletable; this proportion was variable between experiments, ranging between ~20-80%, somewhat regardless of the incubation time (Fig. 5 is typical). Thus, the arrest of NPC assembly at the 'empty pores' stage might be due to a stoichiometric imbalance caused by the partial depletion of complexes that contained p62 or other WGA-binding nucleoporins (see Discussion).

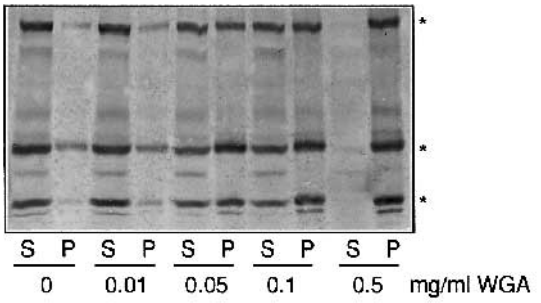

Fig. 5. WGA-binding nucleoporins precipitate when WGA is added to cytosol. WGA at the indicated final concentrations was added to cytosol on ice, incubated for 30 minutes at 22-24°C, and centrifuged. Pellets and supernatants were subjected to SDS-PAGE (5-17% gel), blotted, and probed with WGA (see Materials and Methods). (S) Supernatant; (P) pellet; asterisks indicate positions of p200, p97, and p62, the three major WGA-binding nucleoporins in *Xenopus* eggs.

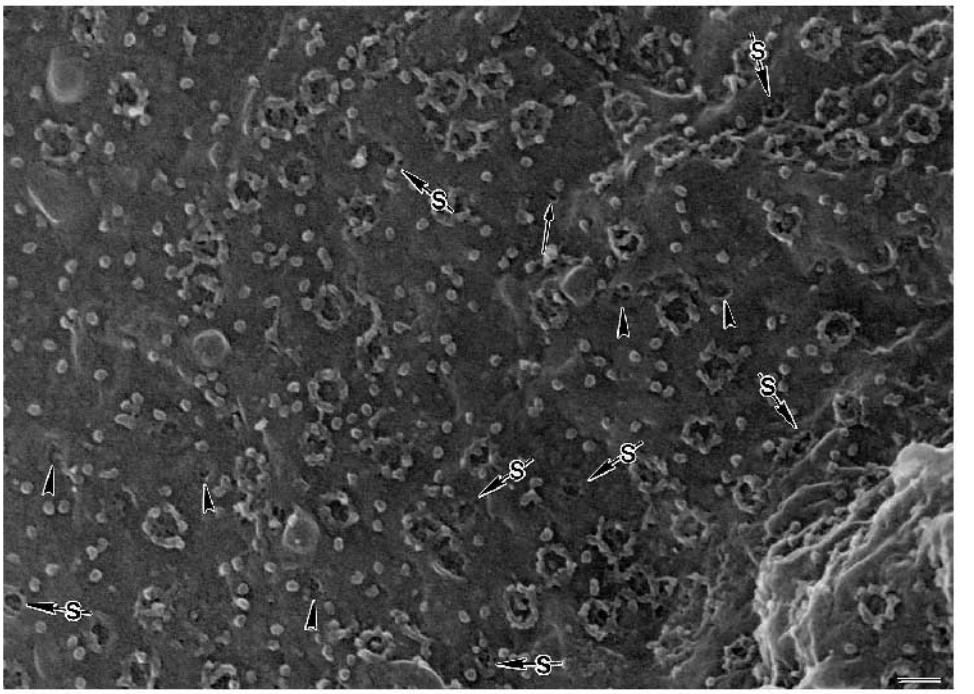

Fig. 6. BAPTA causes star-rings and other intermediates to accumulate. Nuclei were assembled for 50 minutes before adding dibromo-BAPTA; 60 minutes later samples were processed for FEISEM. Star-rings are indicated by arrows marked 's', arrowheads mark stabilizing pores, and the small arrow shows a dimple. Bar, 100 nm.

Dibromo-BAPTA causes star-rings and other structures to accumulate when added 45-50 minutes after initiating assembly

Consistent with the findings of Macaulay and Forbes (1996b), BAPTA completely blocked NPC assembly when added at the beginning of the nuclear assembly reaction (C. Wiese et al., unpublished). To ask if BAPTA also inhibited later stages of NPC assembly, nuclei were assembled normally for up to 50 minutes and then supplemented with 1 mM dibromo-BAPTA for an additional 60 minutes. We used dibromo-BAPTA for these experiments because it is effective at lower concentrations than BAPTA (1 mM versus 5 mM, respectively; Sullivan et al., 1993). Because new NPCs are initiated continuously during the assembly reaction, and because each NPC assembles in less than 8 minutes (C. Wiese et al., unpublished), this strategy yielded nuclei with numerous mature NPCs (completed before dibromo-BAPTA addition), plus other NPCs at various stages of construction (Fig. 6). Many NPC-related structures accumulated when dibromo-BAPTA was added to growing nuclei, but the most dramatic effect was on star-rings. Dibromo-BAPTA-treated nuclear envelopes contained eightfold more star-rings than control nuclei (Table 2): 6.3%, compared to 0.8% star-rings in controls fixed after 40-45 minutes of normal assembly. The proportion of star-rings appeared even greater when dibromo-BAPTA was added as early as 10 minutes after initiating nuclear assembly, with star-rings typically constituting ~10% of total NPC-related structures (data not shown; note that younger nuclei have had less time to accumulate mature NPCs; therefore the proportion of putative intermediates decreases as the inhibitor is added later in assembly, presumably due to the progressive accumulation of mature NPCs). Because star-rings constituted ~1-2% of NPC-related structures in control assembly reactions (Tables 1 and 2), they cannot be simply an artifact of dibromo-BAPTA treatment. Although our results do not eliminate the possibility that dibromo-BAPTA acts by stimulating NPC breakdown, we favor the hypothesis that *ongoing* NPC assembly is arrested by dibromo-BAPTA predominantly at the star-ring stage, and possibly also at other stages. According to this hypothesis star-rings, like stabilizing pores, may be structural intermediates in NPC assembly.

Table 2. Estimated frequency of star-rings in BAPTA-treated and control* nuclei

	Dibromo-BAPTA	Control
Number of star-rings	28	3
Total NPC-related structures	446	358
% Star-rings	6.3%	0.8%

*Control nuclei were assembled for 40-45 minutes and then fixed. Parallel samples were assembled for 45-50 minutes, then dibromo-BAPTA was added, and the nuclei fixed 60 minutes after dibromo-BAPTA addition.

DISCUSSION

We discovered novel features of the growing nuclear envelope: dimples, 'stabilizing pores', and pores filled with distinctive NPC-related structures (star-rings, thin rings). The detection of dimples and pores was probably facilitated by our ability to examine large areas of the outer nuclear membrane at relatively high magnification using FEISEM. Dimples may be difficult to detect by transmission EM, because they were rare and typically too small (~6 nm) to appear convincingly in thin sections (average thickness, 40-60 nm). Previous excellent freeze fracture studies of NPCs did not reveal star-rings or thin rings (Maul, 1977a), perhaps because fracture planes often follow membranes and therefore may not effectively differentiate between these protein structures.

Both star-rings and cytoplasmic thin rings were recently

independently identified as distinct substructures within the mature NPC. Star-rings were discovered by FEISEM examination (Goldberg and Allen, 1996) of *Xenopus* oocyte NPCs whose cytoplasmic ring was physically removed by the method of Unwin and Milligan (1982). The star-ring of mature oocyte NPCs is sandwiched between the spoke ring and the cytoplasmic ring. Consistent with this, we found that star-rings assembled above the central plane of the NPC, and were in turn covered by the thin ring. These data suggested that the thin ring is precursor to the cytoplasmic ring.

Thin rings, which our study showed were not equivalent to the complete cytoplasmic ring (described by Akey and Radermacher, 1993; Goldberg and Allen, 1993) were not previously discovered as a discrete component of NPC structure. However, thin rings were independently recognized and structurally characterized in detergent-extracted mature NPCs from *Chironomus* salivary gland nuclei (E. Kiseleva and T. D. Allen, unpublished data). In the *Chironomus* nuclei, proteolytic dissection revealed the thin ring as the core structural element of the cytoplasmic ring, supporting our conclusion that the thin ring assembled first, and was later overlaid or enwrapped by larger, bulkier structures (see below). These results contribute to the emerging model of NPC structure (Hinshaw et al., 1992; Akey and Radermacher, 1993; Goldberg and Allen, 1996).

In situ construction of individual subunits (modules) of the star-ring, thin ring, and cytoplasmic ring

One important conclusion from this study concerns the modular, stepwise nature of NPC assembly. The 'modules' that we observed were: (a) individual triangular star-ring subunits, which assembled onto the membrane around the edge of the pore; (b) thin ring subunits, which were assembled above the star-ring; and (c) cytoplasmic ring subunits, which formed on and around the thin ring. For any given substructure, such as the star-ring, each of its eight subunits appeared to assemble independently and asynchronously. However, each substructure (e.g. the star-ring) appeared to be complete or nearly-complete before the next phase of construction (e.g. thin ring subunits) was detectable. Our data strongly support a modular model of NPC structure (Unwin and Milligan, 1982; Akey, 1989; Reichelt et al., 1990; Goldberg and Allen, 1996), and further suggest that it might be feasible to assemble NPC substructures such as star-rings in vitro.

A model for NPC assembly: first create and stabilize the pore....

We propose that dimples, 'stabilizing pores', star-rings, and thin rings are intermediates of increasing complexity in NPC assembly, and have ordered them into a hypothetical assembly pathway (Fig. 7). Our first assumption, that these structures were intermediates in assembly rather than disassembly, was based on the efficiency and speed of nuclear assembly in the *Xenopus* extracts, and the stability of mature oocyte NPCs incubated in the extracts (J. M. Cronshaw and M. W. G., unpublished observations). However, we cannot eliminate the possibility that one or more of our putative assembly intermediates actually represents a mis-assembled 'dead end' product. Our second assumption, based on the paradigm of phage assembly, was that smaller, simpler structures are the precursors of larger, more complex structures. Note also that our present observations only account for events at the cytoplasmic surface of the nuclear envelope, and do not reveal events on the nucleoplasmic half of the NPC.

Our results provide evidence that NPC assembly is initiated by a protein-mediated 'bridging' event between the inner and outer nuclear membranes, leading to the formation of the dimple. The geometry of the dimples argued that the integral membrane proteins responsible for dimpling interact through their lumenal domains. (However, our data do not rule out the involvement of soluble nucleoporins in the dimpling event.) Although specific bridging proteins have not yet been identified, the abundant integral pore membrane protein, gp210 (Wozniak et al., 1989; Gerace and Foisner, 1994) is the best candidate. Gp210 has a large lumenal domain that includes a potentially fusogenic hydrophobic 'spur' (Greber et al., 1990) that might be analogous to that of hemagglutinin, a fusogenic viral protein (reviewed by White, 1990). Interestingly, dimpling does not seem to occur in samples exposed to high WGA concentrations. We speculate that 500 μg/ml WGA might interfere with dimpling by binding to the *Xenopus* homolog of POM121, a GlcNac-modified integral membrane pore protein in mammals (Hallberg et al., 1993).

We think that dimpling is evidence that the inner and outer membranes are being brought together so they can fuse, but our present data did not reveal when fusion occurred. For example, the larger dimples might actually be pores. Alternatively, the fusion event that creates the pore might not occur until after the edges of the pore have been stabilized, as hypothesized in Fig. 7.

Based on the variety of shapes of the 'stabilizing pores', we hypothesized that the nascent pore (hole) is stabilized by protein structures that assemble on both the cytoplasmic and lumenal sides of the membrane, forming an interlinked scaffold. This scaffold could involve membrane protein gp210, with its large lumenal domain, and POM121, with its large cytoplasmic domain. The potential involvement of gp210 and POM121 in scaffold formation, dimpling, and membrane fusion needs to be tested experimentally. The assembly of a scaffold might also control the size of the hole, and initiate the assembly of central NPC structures. The central structures within the 'stabilizing pores', which were poorly-resolved in our preparations, nevertheless appeared to be distinct from the NPC basket (which should also be well below the plane of view). These central structures are therefore most likely to represent the spoke ring or part of the central transporter. Alternatively, these central structures might be temporary filters that prevent leakage during NPC assembly.

Regardless of the identity of these central structures, their presence raised an interesting question: during the early stages of NPC assembly, is there a mechanism to prevent leakage across the nuclear envelope? The answer may be 'no', since there is a correlation between higher rates of diffusion into nuclei at times during the cell cycle when the rates of NPC assembly are highest (Maul et al., 1972; Feldherr and Akin, 1990). On the other hand, NPCs assemble during G_2 phase, when the block to rereplication depends on the ability of the nuclear envelope to exclude the cytoplasmic Mcm3 protein ('licensing factor'; Leno et al., 1992; Madine et al., 1995), and leakage might therefore be detrimental. It is also worth considering that if a size-selective filter were installed early in NPC assembly, it must not prevent large components (e.g. see

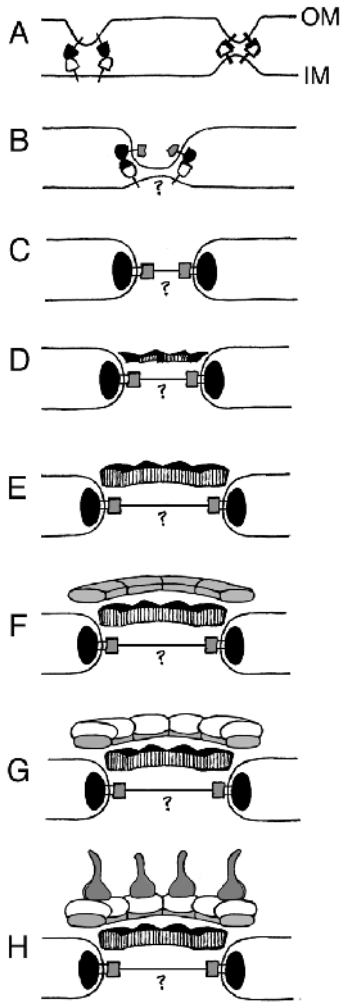

Fig. 7. Working model for NPC assembly in the nuclear envelope. Each intermediate is depicted in cross-section, showing four of the eight symmetric subunits. (A) Stage 1, dimple formation. Two possibilities are shown: one-sided dimpling, and two-sided dimpling. Dimples are proposed to result from the bridging of the inner and outer nuclear membranes by integral membrane pore proteins. (B, C) Stage 2, pore stabilization. At an undetermined stage, depicted here as Stage 2, the inner and outer membranes fuse to form the aqueous pore through the nuclear envelope. (D, E) Star-ring construction. (F) Thin ring construction. (G) Cytoplasmic coaxial ring assembly. (H) Addition of cytoplasmic filaments. Question marks refer to structures not visualized, such as those that face the nucleoplasm, and those in the center of the pore. OM, outer nuclear membrane. IM, inner nuclear membrane.

Guan et al., 1995; Macaulay et al., 1995) from reaching the nucleoplasmic side of the assembling NPC.

...then sequentially assemble the star-ring, thin ring, and cytoplasmic ring

In our hypothetical assembly pathway, dimples are somehow stabilized and converted into pores (holes) with diameters that range from 35-45 nm. As star-ring subunits assembled over the stabilized pore, the pore apparently enlarged further to ~60 nm, suggesting that additional (uncharacterized) central structures had been added or remodelled. Next, a relatively smooth, thin ring assembles on top of the star-ring. We propose that the thin ring is precursor to the cytoplasmic coaxial ring, because the thin ring has the same outer diameter as the cytoplasmic ring but a larger internal diameter. The order of this part of the proposed NPC assembly pathway is based on our observations of individual star-ring modules within the pore, and individual thin ring modules on top of star-rings. Finally, there are likely to be other stages in NPC assembly that we could not detect because they were short-lived, or not distinguishable without the use of molecular markers.

Testing this model

Two structures, stabilizing pores (holes), and pores (holes) containing star-rings, accumulated predominantly when nuclei were assembled in the presence of 50-100 μg/ml WGA, or when growing nuclei were treated with 1 mM dibromo-BAPTA, respectively. These findings support the hypothesis that pores and star-rings are bona fide intermediates in NPC assembly, but do not establish their order within the proposed pathway. Our results show that both WGA and BAPTA will be valuable but non-trivial tools for testing the proposed pathway. BAPTA profoundly inhibits the earliest detectable stages of NPC assembly when present at the start of the reaction (Macaulay and Forbes, 1996b; C. Wiese et al., unpublished). When assembly is allowed to proceed for short times (5-20 minutes) before adding BAPTA, we observe the accumulation of dimples, pores, and other NPC-like structures (C. Wiese and M. W. Goldberg, unpublished observations). As shown here, BAPTA added after 40-50 minutes of assembly caused star-rings to accumulate predominantly, but other structures were also seen. Thus BAPTA appears to arrest NPC assembly at multiple stages, and might be useful in future inhibitor ‘chase’ experiments with WGA.

The inhibitory mechanism of BAPTA and its derivatives is not understood for nuclear assembly reactions. BAPTA was initially thought to inhibit nuclear assembly by buffering Ca^{2+} mobilization events (Sullivan et al., 1993, 1995; see Macaulay and Forbes, 1996b). However in a rigorous test of this hypothesis, we showed using Ca^{2+} ionophores that lumenal Ca^{2+} stores are not required for either nuclear envelope assembly or nuclear import in vitro (Marshall et al., 1997), consistent with previous unpublished in vitro findings by Greber and Gerace (1995). Since mobilizable Ca^{2+} is apparently not involved, our working hypothesis is that BAPTA might directly interfere with certain Ca^{2+}- or Zn^{2+}-binding nucleoporins required for distinct stages in NPC assembly.

WGA can now be used to analyze the structure of ‘empty’ pores, and identify nucleoporins that assemble across the center of the pore. We discovered that WGA has differential concentration-dependent effects on NPC assembly, most notably causing empty pores to accumulate at WGA concentrations that precipitate ~20-80% of the soluble WGA-binding nucleoporin complexes. WGA could arrest NPC assembly at the empty pore stage by at least three mechanisms: (a) by directly binding to pore membrane protein(s) such as POM121; (b) by altering the stoichiometry of one or more soluble WGA-binding nucleoporin complexes; or (c) by binding to nucleoporins after their insertion at the construction site. Several different nucleoporins can disrupt NPCs when overexpressed in vivo (see Davis, 1995), suggesting that nucleoporin stoichiometry is important. However, we are not aware of any haplo-insufficiencies of p62 or other WGA-binding nucleo-

porins that confer a dominant phenotype. We therefore speculate that the empty pore phenotype requires the simultaneous loss or inactivation of more than one type of nucleoporin complex.

It will be interesting to determine when (and where) specific nucleoporins become associated with dimples, stabilizing pores, star-rings, or more complicated structures. In a few cases, the order of assembly of certain nucleoporins is known or suspected from immunofluorescence experiments. For example, ring-shaped p62 complexes associate with the central region of the NPC before one can detect the assembly of Tpr/p270 proteins into intranuclear filaments that attach to the basket (Byrd et al., 1994; Cordes et al., 1997). Although it was previously suggested that some NPC substructures might preassemble on chromatin *before* membrane enclosure (Maul, 1977b; Sheehan et al., 1988) more recent evidence indicates that a double nuclear membrane must form before NPCs can assemble (Macaulay and Forbes, 1996b). Indeed, our data suggest that NPC assembly is initated by events that occur on and within the flattened nuclear membranes; thus, key questions for future investigation are the mechanism and regulation of the membrane fusion event that forms the dimple and 'stabilizing pore'.

We thank Elena Kiseleva and Janet Cronshaw for sharing their unpublished results; Murray Stewart and Elena Kiseleva for their comments; and Sandra Rutherford for her photographic expertise. K.L.W. thanks Alastair Mackay for instruction in Adobe Photoshop. This work was supported by grants from the Human Frontiers Science Program (K.L.W. and T.D.A.), the Council for Tobacco Research, USA (K.L.W.), and the Cancer Research Campaign UK (T.D.A. and M.W.G.).

REFERENCES

Akey, C. W. (1989). Interactions and structure of the nuclear pore complex revealed by cryo-electron microscopy. *J. Cell Biol.* **109**, 955-970.

Akey, C. W. and Radermacher, M. (1993). Architecture of Xenopus nuclear pore complex revealed by three dimensional cryo-electron microscopy. *J. Cell Biol*. **122**, 1-19.

Akey, C. W. (1995). Conformational plasticity of the nuclear pore complex. *J. Mol. Biol*. **248**, 273-293.

Allan, V. J. and Vale, R. (1994). Movement of membrane tubules along microtubules in vitro: evidence for specialized sites of motor attachment. *J. Cell Sci*. **107**, 1885-1895.

Allen, T. D. and Goldberg, M. W. (1993). High resolution SEM in cell biology. *Trends Cell Biol*. **3**, 205-208.

Allen, T. D. and Goldberg, M. W. (1994). High resolution scanning electron microscopy in cell biology. In *Cell Biology: A Laboratory Manual*, vol. 2 (ed. J. E. Celis), pp. 193-202. Academic Press.

Allen, T. D. and Goldberg, M. W. (1995). Four functions and a funeral. *Trends Cell Biol*. **5**, 176-178.

Byrd, D. A., Sweet, D. J., Panté, N., Konstantinov, K. N., Guan, T., Saphire, A. C. S., Mitchell, P. J., Cooper, C. S., Aebi, U. and Gerace, L. (1994). Tpr, a large coiled coil protein whose amino terminus is involved in activation of oncogenic kinases, is localized to the cytoplasmic surface of the nuclear pore complex. *J. Cell Biol*. **127**, 1515-1526.

Cordes, V. C., Reidenbach, S. and Franke, W. W. (1995). High content of a nuclear pore complex protein in cytoplasmic annulate lamellae of Xenopus oocytes. *Eur. J. Cell Biol*. **68**, 240-255.

Cordes, V. C., Reidenbach, S., Rackwitz, H.-R. and Franke, W. W. (1997). Identification of protein p270/Tpr as a major component of the nuclear pore complex-attached intranuclear filaments. *J. Cell Biol*. (in press).

Dabauvalle, M. C., Loos, K. and Scheer, U. (1990). Identification of a soluble precursor complex essential for nuclear pore complex assembly in vitro. *Chromosoma* **100**, 56-66.

Dabauvalle, M. C., Loos, K., Merkert, H. and Scheer, U. (1991). Spontaneous assembly of pore complex-containing membranes ("Annulate Lamellae") in Xenopus egg extract in the absence of chromatin. *J. Cell Biol*. **112**, 1073-1082.

Davis, L. I. (1995). The nuclear pore complex. *Annu. Rev. Biochem*. **64**, 865-896.

Feldherr, C. M. and Akin, D. (1990). The permeability of the nuclear envelope in dividing and nondividing cell cultures. *J. Cell Biol*. **111**, 1-8.

Finlay, D. R. and Forbes, D. J. (1990). Reconstitution of biochemically altered nuclear pores: transport can be eliminated and restored. *Cell* **60**, 17-29.

Finlay, D. R., Meier, E., Bradley, P., Horecka, J. and Forbes, D. J. (1991). A complex of nuclear pore proteins required for pore function. *J. Cell Biol*. **114**, 169-183.

Georgatos, S. D., Meier, J. and Simos, G. (1994). Lamins and lamin-associated proteins. *Curr. Opin. Cell Biol*. **6**, 347-353.

Gerace, L., Ottaviano, Y. and Kondor-Koch, C. (1982). Identification of a major polypeptide of the nuclear pore complex. *J. Cell Biol*. **95**, 826-837.

Gerace, L. and Foisner, R. (1994). Integral membrane proteins and dynamic organization of the nuclear envelope. *Trends Cell Biol*. **4**, 127-131.

Greber, U. F., Senior, A. and Gerace, L. (1990). A major glycoprotein of the nuclear pore complex is a membrane-spanning polypeptide with a large lumenal domain and a small cytoplasmic tail. *EMBO J*. **9**, 1495-1502.

Greber, U. F. and Gerace, L. (1995). Depletion of calcium from the lumen of endoplasmic reticulum reversibly inhibits passive diffusion and signal-mediated transport into the nucleus. *J. Cell Biol*. **128**, 5-14.

Goldberg, M. W. and Allen, T. D. (1992). High resolution scanning electron microscopy of the nuclear envelope: demonstration of a new, regular fibrous lattice attached to the baskets of the nucleoplasmic face of the nuclear pores. *J. Cell Biol*. **119**, 1429-1440.

Goldberg, M. W. and Allen, T. D. (1993). The nuclear pore complex: three dimensional surface structure revealed by field emission, in-lens scanning electron microscopy, with underlying structure uncovered by proteolysis. *J. Cell Sci*. **106**, 261-274.

Goldberg, M. W. and Allen, T. D. (1995). Structural and functional organisation of the nuclear envelope. *Curr. Opin. Cell Biol*. **7**, 301-307.

Goldberg, M. W., Jenkins, H., Allen, T. D., Whitfield, W. G. F. and Hutchison, C. J. (1995). Xenopus lamin B_3 has a direct role in the assembly of a replication competent nucleus: evidence from cell-free egg extracts. *J. Cell Sci*. **108**, 3451-3461.

Goldberg, M. W. and Allen, T. D. (1996). The nuclear pore complex and lamina: three dimensional structures and interactions determined by Field Emission In-lens Scanning Electron Microscopy. *J. Mol. Biol*. **257**, 848-865.

Görlich, D. and Mattaj, I. W. (1996). Nucleocytoplasmic transport. *Science* **271**, 1513-1518.

Guan, T., Müller, S., Klier, G., Panté, N., Blevitt, J. M., Haner, M., Paschal, B., Aebi, U. and Gerace, L. (1995). Structural analysis of the p62 complex, an assembly of O-linked glycoproteins that localizes near the central gated channel of the nuclear pore complex. *Mol. Biol. Cell* **6**, 1591-1603.

Hallberg, E., Wozniak, R. W. and Blobel, G. (1993). An integral membrane protein of the pore membrane domain of the nuclear envelope contains a nucleoporin-like region. *J. Cell Biol*. **122**, 513-521.

Hart, G. W., Haltiwanger, R. S., Holt, G. D. and Kelly, W. G. (1989). Glycosylation in the nucleus and cytoplasm. *Annu. Rev. Biochem*. **58**, 842-874.

Hicks, G. R. and Raikhel, N. V. (1995). Protein import into the nucleus: an integrated view. *Annu. Rev. Cell Dev. Biol*. **11**, 155-188.

Hinshaw, J. E., Carragher, B. O. and Milligan, R. A. (1992). Architecture and design of the nuclear pore complex. *Cell* **69**, 1133-1141.

Hutchison, C. J., Bridger, J. M., Cox, L. S. and Kill, I. R. (1994). Weaving a pattern from disparate threads: lamin function in nuclear assembly and DNA replication. *J. Cell Sci*. **107**, 3259-3269.

Jarnik, M. and Aebi, U. (1991). Toward a more complete 3-D structure of the nuclear pore complex. *J. Struct. Biol*. **107**, 291-308.

Kessel, R. G. (1992). Annulate lamellae: a last frontier in cellular organelles. *Int. Rev. Cytol*. **133**, 43-120.

Kiseleva, E., Goldberg, M. W., Daneholt, B. and Allen, T. D. (1996). RNP export is mediated by structural reorganization of the nuclear pore basket. *J. Mol. Biol*. **260**, 304-311.

Leno, G. H., Downes, C. S. and Laskey, R. A. (1992). The nuclear membrane prevents the replication of human G2 nuclei but not G1 nuclei in Xenopus egg extract. *Cell* **69**, 151-158.

Lohka, M. J. (1988). The reconstitution of nuclear envelopes in cell-free systems. *Cell Biol. Int. Rep*. **12**, 833-848.

Lohka, M. J. and Masui, Y. (1983). Formation in vitro of sperm pronuclei and

mitotic chromosomes induced by amphibian ooplasmic components. *Science* **220**, 719-721.

Lohka, M. J. and Masui, Y. (1984). Roles of cytosol and cytoplasmic particles in nuclear envelope assembly and sperm pronuclear formation in cell-free preparations from amphibian eggs. *J. Cell Biol*. **98**, 1222-1230.

Macaulay, C., Meier, E. and Forbes, D. J. (1995). Differential mitotic phosphorylation of proteins of the nuclear pore complex. *J. Biol. Chem*. **270**, 254-262.

Macaulay, C. and Forbes, D. J. (1996a). Reconstitution of nuclear pore assembly and function. *Semin. Cell Dev. Biol*. **7**, 475-486.

Macaulay, C. and Forbes, D. J. (1996b). Assembly of the nuclear pore: biochemically distinct steps revealed with NEM, GTPγS, and BAPTA. *J. Cell Biol*. **132**, 5-20.

Madine, M. A., Khoo, C. Y., Mills, A. D., Musahl, C. and Laskey, R. A. (1995). The nuclear envelope prevents reinitiation of replication by regulating the binding of MCM3 to chromatin in Xenopus egg extracts. *Curr. Biol.* **5**, 1270-1279.

Marshall, I. C. B., Gant, T. M. and Wilson, K. L. (1997). Ionophore-releasable lumenal Ca^{2+} stores are not required for nuclear envelope assembly or nuclear protein import in Xenopus egg extracts. *Cell Calcium* (in press).

Maul, G. G. (1977a). The nuclear and cytoplasmic pore complex: structure, dynamics, distribution, and evolution. *Int. Rev. Cytol. Suppl.* **6**, 75-186.

Maul, G. G. (1977b). Nuclear pore complexes: elimination and reconstruction during mitosis. *J. Cell Biol.* **74**, 492-500.

Maul, G. G., Maul, H. M., Scogna, J. E., Lieberman, M. W., Stein, G. S., Hsu, B. Y. L. and Borun, T. W. (1972). Time sequence of nuclear pore formation in phytohemagglutinin-stimulated lymphocytes and in HeLa cells during the cell cycle. *J. Cell Biol.* **55**, 433-447.

Maul, H. M., Hsu, B. Y. L., Borun, T. M. and Maul, G. G. (1973). Effect of metabolic inhibitors on nuclear pore formation during the HeLa S_3 cell cycle. *J. Cell Biol*. **59**, 669-676.

Meier, E., Miller, B. R. and Forbes, D. J. (1995). Nuclear pore complex assembly studied with a biochemical assay for annulate lamellae formation. *J. Cell Biol*. **129**, 1459-1472.

Newmeyer, D. D. and Wilson, K. L. (1991). Egg extracts for nuclear import and nuclear assembly reactions. *Meth. Cell Biol*. **36**, 607-634.

Panté, N. and Aebi, U. (1993). The nuclear pore complex. *J. Cell Biol.* **122**, 977-984.

Reichelt, R., Holzenburg, A., Buhle, E. L., Jarnick, M., Engel, A. and Aebi, U. (1990). Correlation between structure and mass distribution of the nuclear pore complex and of distinct pore complex proteins. *J. Cell Biol.* **110**, 883-894.

Ris, H. (1991). The 3D-structure of the nuclear pore complex as seen by high voltage electron microscopy and high resolution low voltage scanning electron microscopy. *EMSA Bull.* **21**, 54-56.

Rout, M. P. and Blobel, G. (1993). Isolation of the yeast nuclear pore complex. *J. Cell Biol*. **123**, 771-783.

Rout, M. P. and Wente, S. R. (1994). Pores for thought: nuclear pore complex proteins. *Trends Cell Biol.* **4**, 357-365.

Sheehan, M. A., Mills, A. D., Sleeman, A. M., Laskey, R. A. and Blow, J. J. (1988). Steps in the assembly of replication-competent nuclei in a cell-free system from Xenopus eggs. *J. Cell Biol.* **106**, 1-12.

Strambio-de-Castillia, C., Blobel, G. and Rout, M. P. (1995). Isolation and characterization of nuclear envelopes from the yeast *Saccharomyces*. *J. Cell Biol*. **131**, 19-31.

Sullivan, K. M. C., Busa, W. B. and Wilson, K. L. (1993). Calcium mobilization is required for nuclear vesicle fusion in vitro: implications for membrane traffic and IP_3 receptor function. *Cell* **73**, 1411-1422.

Sullivan, K. M. C., Lin, D. D., Agnew, W. and Wilson, K. L. (1995). Inhibition of nuclear vesicle fusion by antibodies that block activation of 1,4,5-trisphosphate receptors. *Proc. Nat. Acad. Sci. USA* **92**, 8611-8615.

Ullman, K. S. and Forbes, D. J. (1995). RNA polymerase III transcription in synthetic nuclei assembled in vitro from defined DNA templates. *Mol. Cell. Biol.* **15**, 4873-4883.

Unwin, P. N. and Milligan, R. A. (1982). A large particle associated with the perimeter of the nuclear pore complex. *J. Cell Biol*. **93**, 63-75.

White, J. M. (1990). Viral and cellular membrane fusion proteins. *Annu. Rev. Physiol*. **52**, 675-697.

Wilson, K. L. and Newport, J. (1988). A trypsin-sensitive receptor on membrane vesicles is required for nuclear envelope formation in vitro. *J. Cell Biol*. **10**7, 57-68.

Wilson, K. L. and Wiese, C. (1996). Reconstituting the nuclear envelope and endoplasmic reticulum in vitro. *Semin. Cell Dev. Biol*. **7**, 487-496.

Wozniak, R. W., Bartnik, E. and Blobel, G. (1989). Primary structure analysis of an integral membrane glycoprotein of the nuclear pore. *J. Cell Biol.* **108**, 2083-2092.

Wozniak, R. W., Blobel, G. and Rout, M. P. (1994). POM152 is an integral protein of the pore membrane domain of the yeast nuclear envelope. *J. Cell Biol.* **125**, 31-42.

(Received 6 September 1996 - Accepted 28 November 1996)